A method to recapitulate early embryonic spatial patterning in human embryonic stem cells

Aryeh Warmflash[1–3], Benoit Sorre[1–3], Fred Etoc[1,2], Eric D Siggia[1] & Ali H Brivanlou[2]

Embryos allocate cells to the three germ layers in a spatially ordered sequence. Human embryonic stem cells (hESCs) can generate the three germ layers in culture; however, differentiation is typically heterogeneous and spatially disordered. We show that geometric confinement is sufficient to trigger self-organized patterning in hESCs. In response to BMP4, colonies reproducibly differentiated to an outer trophectoderm-like ring, an inner ectodermal circle and a ring of mesendoderm expressing primitive-streak markers in between. Fates were defined relative to the boundary with a fixed length scale: small colonies corresponded to the outer layers of larger ones. Inhibitory signals limited the range of BMP4 signaling to the colony edge and induced a gradient of Activin-Nodal signaling that patterned mesendodermal fates. These results demonstrate that the intrinsic tendency of stem cells to make patterns can be harnessed by controlling colony geometries and provide a quantitative assay for studying paracrine signaling in early development.

During gastrulation, the cells of the embryo are allocated into three germ layers in an ordered spatial sequence[1]. In mammalian embryos, epiblast cells located on the interior of the embryo migrate to form the definitive endoderm on the outside of the embryo proper and the mesoderm between the endoderm and epiblast. Cells that remain in the epiblast differentiate to ectoderm. Despite the existence of numerous protocols to differentiate hESCs toward cells of these three germ layers[2–5], it is unclear to what degree this spatial order can be recapitulated *in vitro*. Replicating embryonic spatial ordering *in vitro* would allow scientists to investigate, on the molecular level, the intercellular communication that is responsible for embryonic patterning in the human system. This would also be an important step toward generating spatially ordered tissues for clinical purposes.

Studies in fish, frog and mouse embryos have established that spatial patterning during gastrulation is under the control of the Activin-Nodal, BMP and WNT pathways. In both mouse embryos and embryoid bodies derived from mouse embryonic stem cells, these three pathways form a positive feedback loop that establishes polarity[6,7]. The same three pathways can be manipulated to differentiate hESCs to any of the three germ layers[2–5]. However, because these protocols have been optimized to yield pure populations, it is unclear whether stem cells are capable of faithfully generating early embryonic patterns. Simple application of growth factors tends to produce multiple fates without inducing consistent spatial order[8,9]. Previous studies using control of colony geometries noted a shift in the proportion of cells adopting different fates as the colony size was changed but did not observe spatial organization[10–12].

Here we show that cells confined to circular micropatterns and differentiated with BMP4 produce an ordered array of germ layers along the radial axis of the colony. This order results from self-organized signaling that confines response to the BMP4 to the colony border while inducing a broader gradient of Activin-Nodal signaling to pattern mesendodermal fates. Control of fates is established from the border of the colony so that as colony size is reduced, the central fates are lost. Thus, given minimal geometric and signaling cues, hESCs will self-organize to generate embryonic patterns.

RESULTS

Prepatterning in pluripotent hESC colonies

We investigated whether hESCs could give rise to spatially ordered germ layers. We focused on differentiating cells with BMP4 ligand because it represents an early step in the embryonic signaling cascade that initiates gastrulation[1,6]. hESCs rapidly differentiate in response to BMP4, in contrast to Activin-Nodal and WNT signaling, both of which also play a role in the pluripotent state[9,13–15]. The results of BMP4 treatment on hESCs have been controversial: some groups have reported differentiation to trophectoderm[16–19], whereas others have reported a mixture of embryonic and extra-embryonic mesoderm[20].

Under standard culture conditions, hESCs grew in colonies that exhibited a wide range of sizes and shapes (**Fig. 1a**). Differentiation of embryonic stem cells with BMP4 led to spatial patterns of differentiation that differed drastically between neighboring colonies (**Supplementary Fig. 1**). We hypothesized that the heterogeneity in colony geometries could affect cell-cell signaling and result in a loss of reproducible spatial order upon differentiation. We therefore evaluated the effects of using micropatterned technology to grow cells in colonies of precisely controlled size and geometry (**Fig. 1b**).

[1]Center for Studies in Physics and Biology, The Rockefeller University, New York, New York, USA. [2]Laboratory of Molecular Vertebrate Embryology, The Rockefeller University, New York, New York, USA. [3]These authors contributed equally to this work. Correspondence should be addressed to E.D.S. (siggiae@rockefeller.edu) or A.H.B. (brvnlou@rockefeller.edu).

RECEIVED 23 OCTOBER 2013; ACCEPTED 19 MAY 2014; PUBLISHED ONLINE 29 JUNE 2014; DOI:10.1038/NMETH.3016

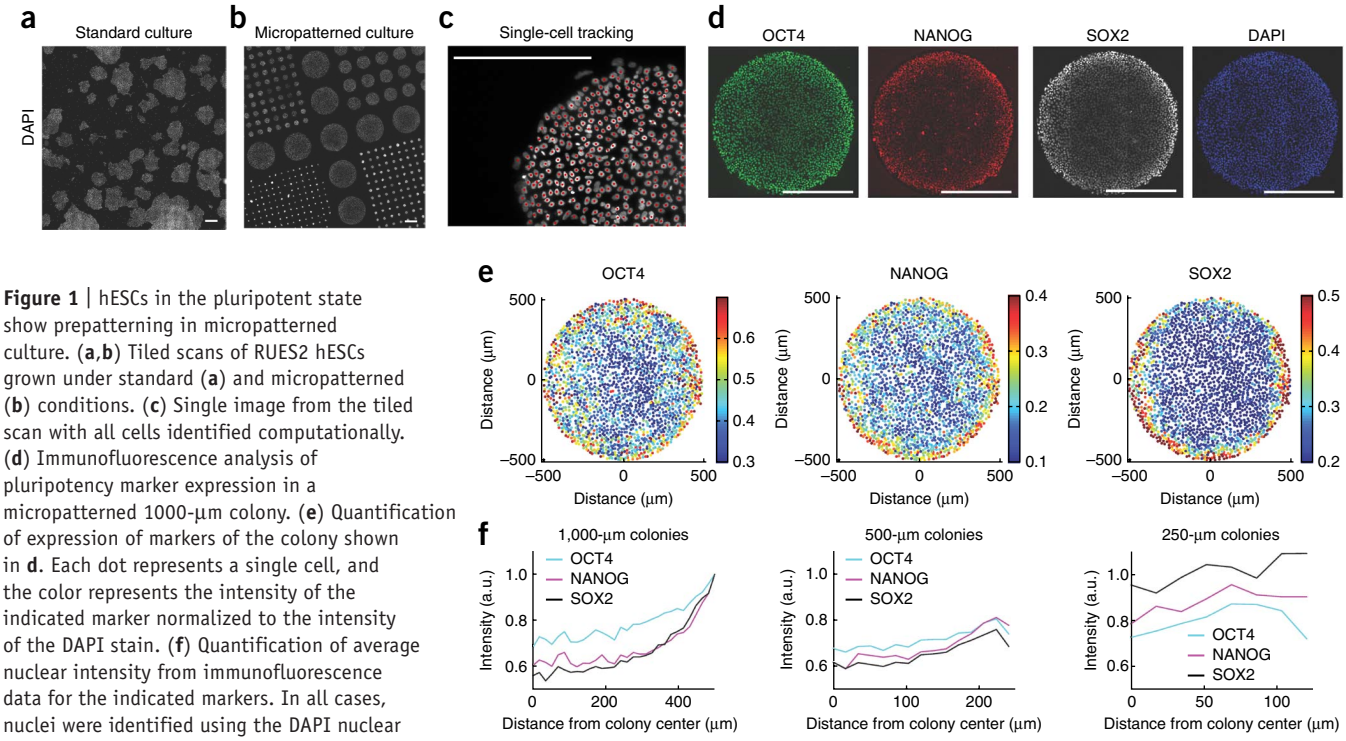

Figure 1 | hESCs in the pluripotent state show prepatterning in micropatterned culture. (**a**,**b**) Tiled scans of RUES2 hESCs grown under standard (**a**) and micropatterned (**b**) conditions. (**c**) Single image from the tiled scan with all cells identified computationally. (**d**) Immunofluorescence analysis of pluripotency marker expression in a micropatterned 1000-μm colony. (**e**) Quantification of expression of markers of the colony shown in **d**. Each dot represents a single cell, and the color represents the intensity of the indicated marker normalized to the intensity of the DAPI stain. (**f**) Quantification of average nuclear intensity from immunofluorescence data for the indicated markers. In all cases, nuclei were identified using the DAPI nuclear counterstain, and the intensity of the indicated markers was normalized to the DAPI intensity. In this and all other figures, graphs represent the mean of 25, 144 and 576 colonies for the colonies of diameters 1,000, 500 and 250 μm, respectively. s.d. between colonies is shown in **Supplementary Figure 3**. Each marker was quantified in two independent experiments. a.u., arbitrary units. Scale bars, 500 μm.

hESCs grown on micropatterns for 24 h in pluripotency conditions maintained pluripotent morphology and expression of markers OCT4, SOX2 and NANOG (**Fig. 1d**). We computationally identified all cells in a large number of colonies (throughout the manuscript, $n = 25$, 144, and 576 for colonies 1,000, 500 and 250 μm in diameter, respectively) (**Fig. 1c**). In the largest colonies, pluripotency markers were uniformly expressed over the center of the colony but rose toward the edges over a range of approximately 150 μm (**Fig. 1e**,**f**).

Signaling pathway activity for the BMP, Activin-Nodal and Wnt pathways as measured by the activity of the SMAD1/5/8, SMAD2/3 and β-catenin signal transducers, respectively, were all elevated toward the edges of the colonies as well (**Supplementary Fig. 2**). In intermediate-sized colonies (500-μm diameter), the size of the region of elevated expression was approximately the same. Colonies 250 μm and smaller uniformly expressed the pluripotency markers at the levels of the cells at the edges of larger colonies (**Fig. 1f**). These trends were observed in nearly every colony (**Supplementary Fig. 3**). These results reveal a previously unappreciated spatial ordering in pluripotent hESC colonies: the edges of colonies differ from their centers, and control of this difference is exerted from the edge inwards. As a result, small colonies are equivalent to the edges of large colonies with respect to signaling pathway activity and expression of pluripotency factors.

Spatial ordering in differentiated micropatterned colonies

Treatment of micropatterned hESC colonies with 50 ng/ml BMP4 led to morphological differentiation within 24 h of treatment, with a dense ring of cells forming at a reproducible radius within the colony with larger, more spread cells radially to the inside and outside (**Fig. 2a**). We next examined whether the reproducible cell geometries led to organized germ layer differentiation.

Transcription factors that are essential for pluripotency are reused during differentiation in order to both activate and repress lineage-specific factors[21–24]. Following the spatial dynamics of pluripotency markers can thus aide in the identification of germ layers. SOX2 expression is specifically maintained during ectodermal differentiation but downregulated during mesendodermal differentiation, whereas OCT4 and NANOG follow the opposite pattern. After 42 h of micropatterned differentiation, SOX2 was expressed only at the center of the 1,000-μm colonies (**Fig. 2a**). This pattern resulted from a dramatic rise in SOX2 protein levels while OCT4 and NANOG were downregulated in this region (**Supplementary Fig. 4**). The elevated SOX2 expression and the exclusion of NANOG, Brachyury (BRA), Eomesodermin (EOMES), SOX17 and Nodal signaling identifies the center with prospective ectoderm[22]. Markers that would distinguish subpopulations of the ectoderm such as Keratin 14 for epidermal cells and PAX6 or SOX1 for neural cells arise only later in development[5,25].

Moving outward from the center region, there was a ring of BRA expression (**Fig. 2a**). This ring also expressed NANOG and OCT4 but not SOX2, which represses mesendodermal fates[23,24] (**Supplementary Fig. 5**). Much of this region also expressed the mesendodermal markers EOMES and GATA6, but these markers extended further away from the colony center along the radial axis (**Fig. 2b** and **Supplementary Fig. 5**). Many of the cells in this region also expressed CDX2, which was expressed in a broad domain that extended to the colony border. At the level

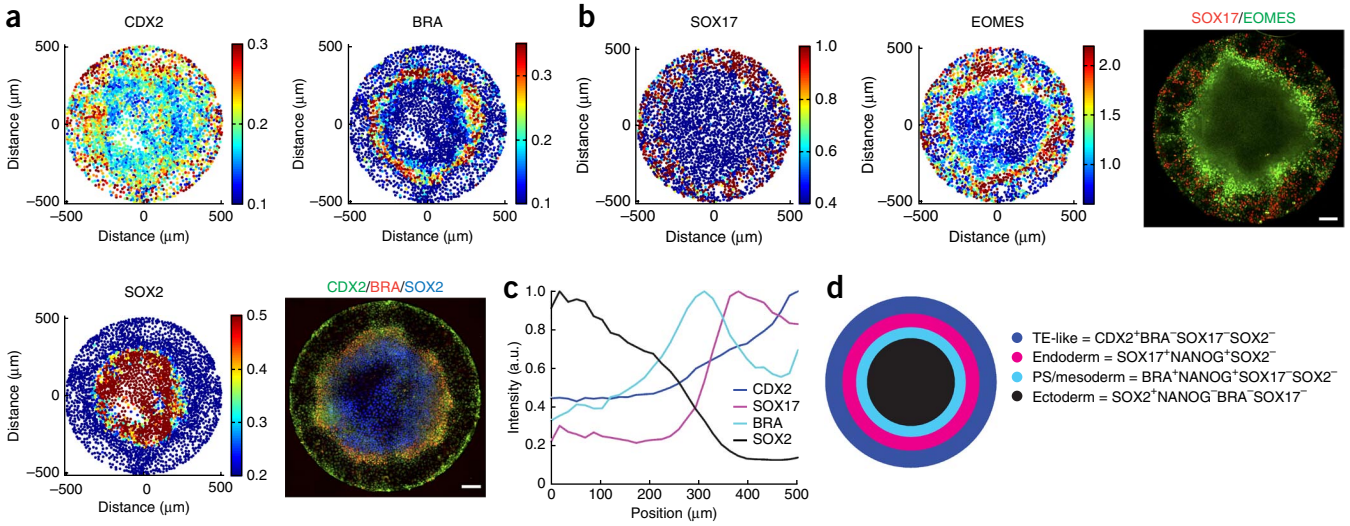

Figure 2 | hESCs differentiated on micropatterns form self-organized spatial patterns. (**a**,**b**) The plots show quantified immunofluorescence data for the indicated fate markers. Cells were seeded on micropatterned coverslips, grown overnight and then treated with BMP4 for 42 h. In **a** and **b**, all plots show data for the same colony. Each dot corresponds to a single cell. The bottom right panel in **a** and the right panel in **b** show an immunofluorescence image of the colony quantified in the plots. (**c**) Quantification of the mean across colonies of immunofluorescence data for germ layer markers. Numbers of colonies are as in **Figure 1f**. Error bars for these and other markers can be found in **Supplementary Figure 5**. Each marker was quantified in three independent experiments. a.u., arbitrary units. (**d**) Schematic of the results of 42 h of BMP4 treatment in micropatterned culture. TE, trophectoderm; PS, primitive streak. Scale bars, 100 μm.

of individual cells, CDX2, EOMES and NANOG were all coexpressed with BRA (**Supplementary Figs. 6a–c** and **7a**,**b**), whereas SOX2 was mutually exclusive with all of these markers (**Supplementary Fig. 6d**,**e**). This set of observations is consistent with the identification of this region as primitive streak and nascent mesodermal cells.

Beyond the ring of BRA expression, we found cells expressing the definitive endoderm marker SOX17 (**Fig. 2b**). Its expression overlapped with the outer ridge of the cells that were positive for EOMES or GATA6 staining but extended further along the radial axis of the colony (**Fig. 2b** and **Supplementary Fig. 6g**). Many of the cells expressing SOX17 also expressed high levels of NANOG, consistent with a role of NANOG in endodermal differentiation[23] (**Supplementary Fig. 7c**,**d**). No expression of SOX2 was detected in this population (**Supplementary Fig. 6f**).

Finally, we observed a broad ring of CDX2 expression that peaked at the very edge of the colony but extended through the mesendodermal region. The coexpression of CDX2 and BRA (**Supplementary Fig. 6a**) is consistent with expression of CDX2 in the mesoderm[26]; however, the outermost cells of the colony expressed CDX2 without expression of mesendodermal markers BRA, SOX17 and GATA6 or pluripotency markers OCT4, NANOG and SOX2 (**Supplementary Figs. 5** and **6**). These outer cells were positioned corresponding to the extraembryonic tissue in the embryo that surrounds the epiblast, and they also displayed high BMP signaling (see below) similar to the trophoectoderm in the embryo[1]. These cells expressed EOMES, but at lower levels than in the mesendoderm (**Supplementary Fig. 6c**). The cells at the colony edge thus shared many characteristics with extraembryonic trophoblast cells, but the true identity of trophoblast-like cells induced by BMP4 remains the subject of debate in the literature[17–20]. In sum, we found that cells confined to circular geometries and incubated with BMP4 differentiated to all three germ layers and a trophoblast-like population in an ordered sequence along the radial axis of the colony (**Fig. 2c**,**d**).

The radial structure of the patterns was extremely reproducible (**Supplementary Figs. 5** and **8**). There remained small angular inhomogeneities (for example, as seen in **Figure 2a** and **Supplementary Fig. 7a**,**c**) that correlated with cell density and were impossible to control during cell seeding. We found very similar patterns for two additional hESC lines, RUES1 and H1 (**Supplementary Fig. 9a**,**b**). We also found similar patterns if cells were grown on recombinant Laminin-521 instead of Matrigel or if they were grown in mTeSR1 medium instead of conditioned medium (**Supplementary Fig. 9c**,**d**). Thus, forcing cells to grow in a confined geometry triggered spontaneous emergence of embryonic patterning in three hESC lines and under all conditions examined.

Gastrulation-like events in micropatterned differentiation

The expression of BRA and the emergence of all three germ layers in the micropatterned cultures suggested that cells might be patterned by gastrulation-like events in a region resembling the primitive steak. In the embryo, FGF signaling in the primitive streak leads to cells undergoing an epithelial-to-mesenchymal transition (EMT), upregulating the transcription factor SNAIL and downregulating or removing E-cadherin (E-CAD) from the cell surface[1]. Indeed, in micropatterned culture, the downstream effector of FGF signaling, phospho-ERK, was primarily localized to the region of BRA expression (**Fig. 3a**). We also observed upregulation of SNAIL in this region (**Fig. 3b**), and E-CAD was internalized, becoming more cytoplasmic rather than being exclusively localized to the cell membrane[27] (**Fig. 3c**).

To better understand these gastrulation-like processes, we examined the three-dimensional (3D) structure of the colonies. 3D reconstruction of the colonies based on 4,6-diamidino-2-phenylindole (DAPI) staining revealed that at the inside and outside

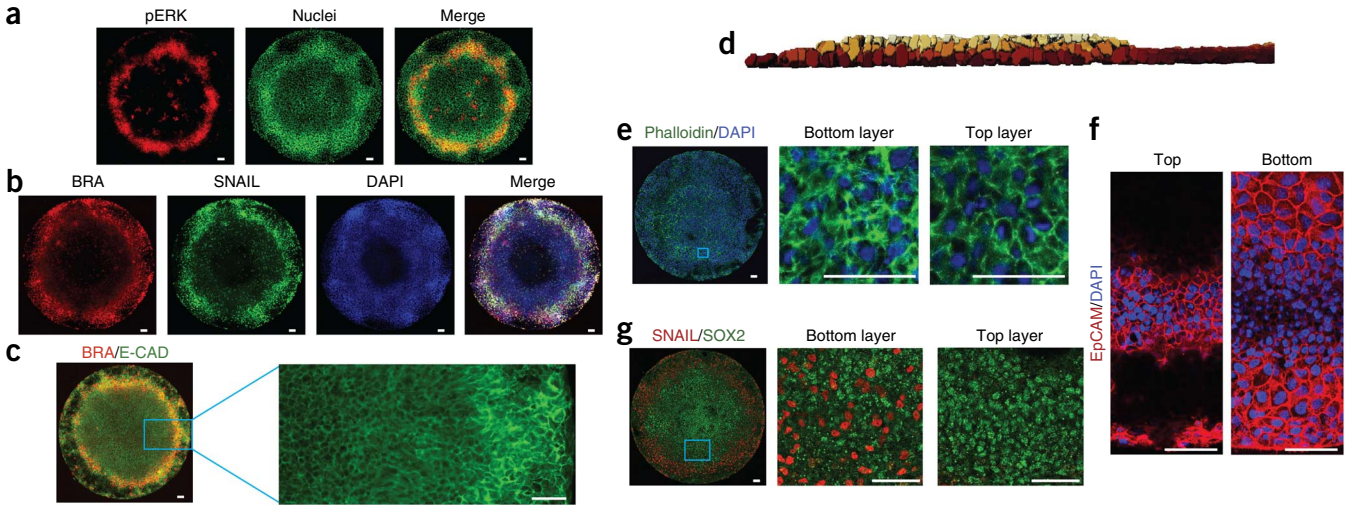

Figure 3 | During differentiation, hESCs undergo an epithelial-to-mesenchymal transition in a region expressing markers of the primitive streak. (**a**–**c**) Immunofluorescence staining of an hESC colony for the indicated markers. The magnified image in **c** shows only the E-CAD stain, for clarity. (**d**) 3D reconstruction of the primitive streak–like region. 3D segmentation of the DAPI image was performed using custom software written in Matlab, and the resulting segmented nuclei were visualized with Imaris. The cells are color coded according to their position in the *z* direction for ease of visualization. (**e**–**g**) Phalloidin staining and immunofluorescence staining for the indicated markers in the upper and lower layers of the primitive streak–like region. In **e** and **g**, the blue boxes (left) indicate the region expanded in the individual confocal slices (center and right). Each panel in **f** is an individual confocal slice. EpCAM, epithelial cell adhesion molecule. Scale bars, 50 μm.

of the colonies, the cells grew as a monolayer, whereas inside the primitive streak–like region, cells were piled two or three layers deep (**Fig. 3d**). We next examined the actin cytoskeleton using phalloidin and found that in the monolayered regions, as well as in the upper layer of the streak-like region, the actin was largely localized to the cell membranes, consistent with the entire top of the colony forming an epithelial layer. In the streak-like region, cells in the bottom layers displayed a more active cytoskeleton consistent with migratory cells that have undergone an EMT (**Fig. 3e**). In agreement with this interpretation, the entire top of the colony expressed the epithelial cell adhesion molecule, EpCAM[28], on the cell membranes, whereas cells in the lower layer of the streak-like region did not (**Fig. 3f**). Where the colonies were multiple layers thick, cells in the lower layers expressed SNAIL, whereas those in the upper layer expressed SOX2 (**Fig. 3g**). We also found individual SNAIL-expressing cells under the epithelial layer closer to the colony center (**Fig. 3g**), which likely represent cells that underwent EMT at the streak-like region and then migrated under the epithelial layer of the colony. Taken together, these results suggest that cells in the BRA-expressing region undergo EMT and migrate inwards toward the surface of the culture dish and then underneath the upper epithelial layer, mimicking human gastrulation movements.

Patterns are controlled from the colony edge

We next examined the differentiation patterns as a function of colony size. The edges of all colonies expressed the same markers at the same radial distance from the colony edge, irrespective of colony size. As the colony size decreased, the SOX2-expressing population at the interior of the colonies was lost (**Fig. 4a**,**b**), whereas the territory of mesodermal differentiation extended to the center of the colony (**Fig. 4c**,**d**), forming a disk rather than an annulus. Examined at the level of single cells, reductions in colony size caused a shift away from SOX2$^+$ ectodermal cells and toward NANOG$^+$ mesendodermal derivatives. In colonies 250 μm and below, no SOX2 expression remained (**Fig. 4b**). Thus, our data show that the differentiation patterns arise via a mechanism that senses the exterior edge of the colony.

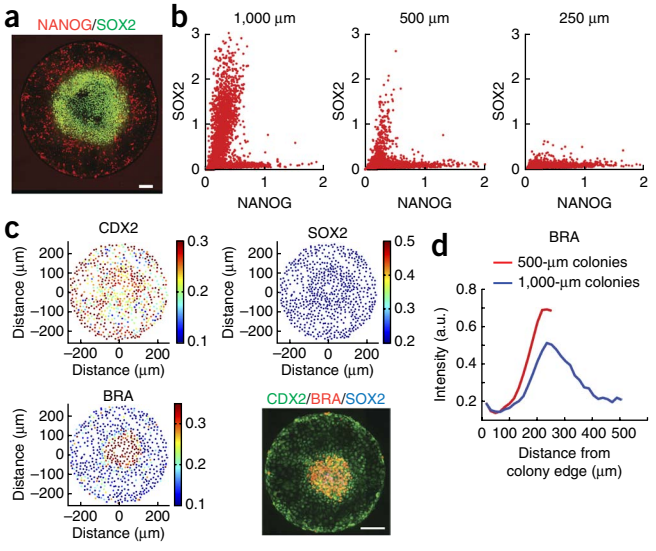

Figure 4 | Control of cell fate extends from the edge of the colony. (**a**) Immunofluorescence for SOX2 and NANOG in a 1,000-μm colony following 42 h of BMP4 treatment. (**b**) Quantification of single-cell expression of SOX2 and NANOG from immunofluorescence data in colonies of different size. (**c**) Immunofluorescence of the indicated markers in a 500-μm colony (bottom right) and quantified marker expression with single-cell resolution. (**d**) Comparison of BRA expression between 500-μm and 1,000-μm colonies. Plots show mean across colonies (n = 25 for 1,000 μm and n = 144 for 500 μm). This experiment was performed three times. Note the distance scale is inverted relative to previous panels to emphasize control from the boundary. a.u., arbitrary units. Scale bars, 100 μm.

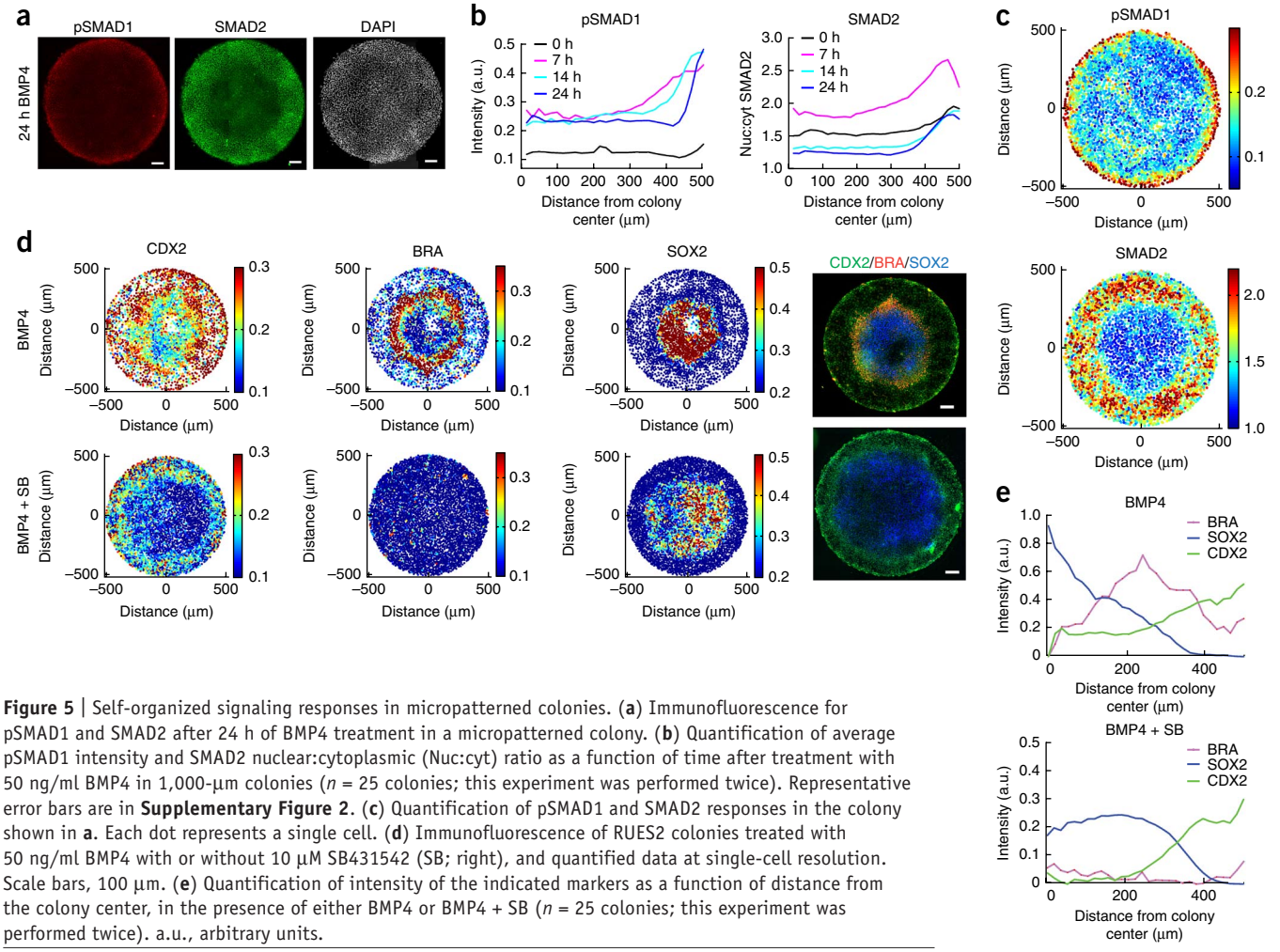

Figure 5 | Self-organized signaling responses in micropatterned colonies. (**a**) Immunofluorescence for pSMAD1 and SMAD2 after 24 h of BMP4 treatment in a micropatterned colony. (**b**) Quantification of average pSMAD1 intensity and SMAD2 nuclear:cytoplasmic (Nuc:cyt) ratio as a function of time after treatment with 50 ng/ml BMP4 in 1,000-μm colonies (n = 25 colonies; this experiment was performed twice). Representative error bars are in **Supplementary Figure 2**. (**c**) Quantification of pSMAD1 and SMAD2 responses in the colony shown in **a**. Each dot represents a single cell. (**d**) Immunofluorescence of RUES2 colonies treated with 50 ng/ml BMP4 with or without 10 μM SB431542 (SB; right), and quantified data at single-cell resolution. Scale bars, 100 μm. (**e**) Quantification of intensity of the indicated markers as a function of distance from the colony center, in the presence of either BMP4 or BMP4 + SB (n = 25 colonies; this experiment was performed twice). a.u., arbitrary units.

We studied the dynamics of how these patterns emerge in colonies of various sizes and found that the markers CDX2, BRA, SOX17 and EOMES all showed initial expression at the colony border and then moved inwards as a function of time, to varying degrees (**Supplementary Fig. 4**). In contrast, SOX2 expression rose continually at the colony center while declining at the colony border. These data suggest that either the primitive streak–like region moves through the colony in time, a process that may result from the spatial confinement, or that cells begin expressing differentiation markers before entering the primitive streak–like region. Examination of different colony sizes revealed identical dynamics of patterning as measured from the colony edge inwards for all markers examined: CDX2, BRA, EOMES, SOX17, SNAIL and SOX2 (**Supplementary Fig. 10**). This demonstrates that patterning has a fixed length scale and proceeds identically in time, regardless of the size of the colony.

Patterns originate in self-organized signaling responses

The ability of BMP4 ligand to generate these patterns is surprising because BMP4 was presented homogeneously at high doses to all cells. To examine the origins of the self-organized differentiation, we determined SMAD1/5/8 status—a proximal readout of BMP signaling—as a function of time (**Fig. 5a–c**). The initial response was highest at the colony edge, with some patches of response in the center. Signaling became increasingly restricted to the colony edge over time. At 24 h after the application of the BMP4 ligand, elevated signaling was largely confined to a narrow ring at the colony edge (**Fig. 5a–c**). Thus, prolonged BMP4 signaling at the colony border likely specifies the extraembryonic fates found there (which is consistent with the expression of BMP4 in extraembryonic tissue in the mouse embryo[1]).

As Activin-Nodal signaling functions downstream of BMP4 in the mouse embryo and is crucial for specifying mesendodermal derivatives, we reasoned that these signals may pattern the mesendoderm in our micropatterned colonies as well. Indeed, a gradient of nuclear SMAD2 formed across the colony, and by 7 h it spanned the range of the future mesendoderm, peaking in the endoderm (**Fig. 5a–c**). To determine the relevance of this gradient for patterning, we inhibited Activin-Nodal signaling with the small molecule SB431542 (ref. 29) during BMP4-mediated differentiation. SB431542 completely inhibited mesendodermal differentiation, as reflected by an absence of BRA$^+$ and SOX17$^+$ cells. Under these conditions, the entire colony could be divided into two territories: CDX2$^+$ extraembryonic cells and SOX2$^+$ ectodermal cells (**Fig. 5d**). These results indicate that in the absence of Activin-Nodal signaling, cells make a binary fate choice likely based on the level of response to the BMP4 signal. BMP signaling thus specifies a range of fates by inducing CDX2$^+$ cells at the colony border while also inducing an Activin-Nodal signaling gradient that induces

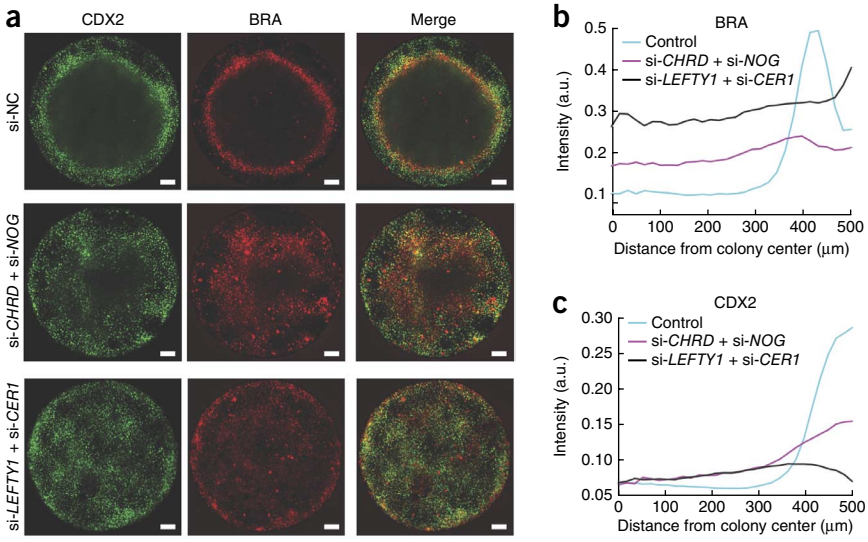

Figure 6 | TGF-β inhibitors are required for pattern formation. (**a**) Immunofluorescence staining of a 1,000-μm micropatterned colony for the indicated markers, when transfected with a nontargeting siRNA (si-NC) or upon specific gene knockdown. Scale bars, 100 μm. (**b**,**c**) Quantification of the mean across colonies (n = 25) of BRA (**b**) and CDX2 (**c**). This experiment was performed twice. a.u., arbitrary units.

mesendodermal fates. Cells at the center of the colony that do not receive either of these signals adopt an ectodermal fate.

These results also shed light on discrepancies in previous data regarding the outcome of BMP-mediated differentiation[16,20]. Note that the range of CDX2 expression extended from the colony border and encompassed BRA$^+$ cells as well as the trophoblast-like cells at the border (**Supplementary Fig. 11**). Thus, there are at least two populations of CDX2$^+$ cells at spatially distinct locations: (i) a population that overlaps with BRA expression and represents embryonic mesoderm or primitive streak and (ii) a BRA$^-$ population at the edge of the colonies that is suggestive of its extraembryonic expression[1]. Notably, treatment with SB431542 both abolished BRA staining and diminished the range of CDX2 expression (**Fig. 5d**,**e**), further confirming that the CDX2$^+$ population that overlaps with BRA expression is mesodermal and that the CDX2$^+$ population at the colony edge is not. The ability to segregate and manipulate these two populations highlights the power of the micropatterning approach for understanding differentiation by providing spatial context.

TGF-β and BMP inhibitors are required for pattern formation

How is the differential response to exogenously supplied BMP established within the colony? The fact that signaling was highest at the colony edge suggests that a diffusible inhibitor that is lost from the colony edge, and thus assumes its highest level in the center, might be responsible for forming these patterns. In the mouse embryo the double knockout of the genes encoding BMP inhibitors Chordin and Noggin shows a loss of the forebrain as a result of expanded BMP signaling[30]. To test whether these genes are involved in the differential response to BMP, we used siRNA to reduce their expression in this human system. Consistent with the knockout phenotype, knockdown caused expansion of mesodermal markers into the ectodermal territory in the center (**Fig. 6**). We used a similar strategy to determine whether Activin-Nodal inhibitors are necessary to restrict activity to the primitive streak–like region. In the mouse embryo, the combined activities of Lefty1 and Cer1 are required to restrict the primitive streak to one side of the embryo[31]. In micropatterned culture, knockdown of *LEFTY1* and *CER1* with siRNA also caused an expansion of the BRA-expressing cells into the ectodermal territory (**Fig. 6a**,**b**). In contrast to the knockdown of the BMP inhibitors, the region of BRA expression also expanded into the region of CDX2$^+$BRA$^-$ cells that typically forms at the colony border, and CDX2 expression at the colony border was diminished (**Fig. 6**). These results demonstrate that inhibitors to the BMP pathway are necessary to preserve the ectodermal character of the colony center, and those of the Activin-Nodal branch are necessary to restrict the primitive streak–like region from both sides. These experiments also provide proof of principle that micropatterned culture can be used to study the effects of genetic perturbations on spatial patterning in the human system.

Consistent with a role for diffusible inhibitors in establishing patterns, blocking diffusion out of the colony by growing cells at the bottom of a PDMS microwell prevented the formation of boundary fates. We observed an absence of staining for trophoectodermal or mesendodermal markers CDX2, BRA, EOMES and SOX17 in colonies grown within microwells; instead nearly all cells stained positively for SOX2 (**Supplementary Fig. 12**). Control cells in the same culture dish but outside of the microwells established patterns containing all three germ layers. These results suggest that geometric control of paracrine signaling could also be used to enhance the purity of stem cell derivatives.

DISCUSSION

Our results show that simple confinement of hESCs to a disk-shaped region is sufficient to recapitulate much of germ layer patterning. The human epiblast is a disk-shaped epithelium at gastrulation, and the cup-like mouse embryo is often approximated as a disk[32,33]. The number of cells in mammalian embryos at this stage is comparable to that in our larger disks. Thus, cells grown on patterned substrates are a sensible approximation to the early gastrula and more appropriate than a solid embryoid body.

A number of groups have attempted to control spatial aspects of stem cell organization during differentiation and have shown that colony size can influence the proportions of fates achieved[10,11]. However, these studies mostly focused on alternate differentiation protocols (for example, withdrawal of pluripotency conditions) and did not find spatial ordering upon differentiation. 3D culture systems have also been devised with no reports of spontaneous, reproducible spatial organization[34].

Colony structure is shaped by inhibitors much as in the embryo. They likely leak from the colony boundary, as evidenced by the loss of edge fates when colonies are grown inside a microwell. The boundary is thus a reference point from which diffusion of ligands and inhibitors define germ layer territories of fixed size.

The micropattern has a secondary consequence of increasing cell density and thus favoring cell communication over response to the external differentiation stimulus. In contrast to micropatterned culture, the SOX2 levels at the colony center never increase over their pluripotent values for BMP4 differentiation under standard culture conditions, a fact we attribute to lower levels of inhibitors produced or transmitted at lower cell densities. It will be interesting to probe the physical mechanisms of cell communication with a gentle flow over the colonies[35].

Recently, self-organized organogenesis has received much attention with reports of the ability to generate optic cups[36], brain-like organoids[37] and mini-guts[38–40] *in vitro* starting from embryonic stem cells. These studies employ primarily chemical cues rather than geometric confinement. Thus it will be interesting to see what effects spatial confinement has on later stages of differentiation. Quantitative models of signaling derived from disk geometry could potentially be used to engineer more reproducible organoids.

Developmental biologists have made great strides by connecting genetic perturbations with defects in spatial patterning. In the future, micropatterned differentiation will allow the same manipulations to be performed for the early stages of hESC differentiation. We provide a proof of principle for this approach by determining the spatial patterning phenotypes of knocking down gene products with siRNA. The advent of clustered, regularly interspaced, short palindromic repeats (CRISPR) technology will allow for the same assay to be performed with complete gene knockouts. The micropatterned colonies will facilitate time-lapse imaging of reporters for dynamic studies and provide an assay for mechanistic questions that are difficult to address in a mammalian embryo. When do the mesodermal and endodermal populations begin to diverge? What combination of geometric or genetic spatial symmetry breaking is needed to induce the anterior-posterior embryonic axis? Can extraembryonic tissue be replaced with signals applied directly on the epiblast? None of the current standards of embryonic stem cell culture is capable of addressing these issues quantitatively. Other applications of micropatterned differentiation include interspecies comparisons, as well as comparison between human induced pluripotent stem cells and hESCs, under similar assay conditions. As the patterns arise in a self-organized manner, micropatterned stem cell culture also provides a novel, controlled platform for studying how signaling generates developmental patterns. We thus propose that geometrically controlled cell culture should become standard practice for embryonic stem cell differentiation.

METHODS

Methods and any associated references are available in the online version of the paper.

Note: Any Supplementary Information and Source Data files are available in the online version of the paper.

ACKNOWLEDGMENTS

The authors are grateful to S. Li and A. Yoney for technical assistance, C. Kirst for assistance with 3D image segmentation, and members of the A.H.B. and E.D.S. laboratories, A.-K. Hadjantonakis and S. Nowotschin for helpful discussions. Funding supporting this work was provided by The Rockefeller University, NYSTEM, US National Institutes of Health grants R01 HD32105 (to A.H.B.) and R01 GM 101653 (to A.H.B. and E.D.S.), US National Science Foundation grant PHY-0954398 (to E.D.S.) and the Human Frontier Science Program LT000851/2011-l (to B.S.).

AUTHOR CONTRIBUTIONS

A.W. designed and performed experiments, performed analysis and wrote the paper. B.S. designed and performed experiments and contributed to writing the paper. F.E. performed experiments and contributed to writing the paper. E.D.S. designed experiments, performed analysis and wrote the paper. A.H.B. designed experiments and wrote the paper.

COMPETING FINANCIAL INTERESTS

The authors declare no competing financial interests.

1. Arnold, S.J. & Robertson, E.J. Making a commitment: cell lineage allocation and axis patterning in the early mouse embryo. *Nat. Rev. Mol. Cell Biol.* **10**, 91–103 (2009).
2. D'Amour, K.A. *et al.* Efficient differentiation of human embryonic stem cells to definitive endoderm. *Nat. Biotechnol.* **23**, 1534–1541 (2005).
3. Chambers, S.M. *et al.* Highly efficient neural conversion of human ES and iPS cells by dual inhibition of SMAD signaling. *Nat. Biotechnol.* **27**, 275–280 (2009).
4. Kattman, S.J. *et al.* Stage-specific optimization of Activin/Nodal and BMP signaling promotes cardiac differentiation of mouse and human pluripotent stem cell lines. *Cell Stem Cell* **8**, 228–240 (2011).
5. Ozair, M.Z., Noggle, S., Warmflash, A., Krzyspiak, J.E. & Brivanlou, A.H. SMAD7 directly converts human embryonic stem cells to telencephalic fate by a default mechanism. *Stem Cells* **31**, 35–47 (2013).
6. Ben-Haim, N. *et al.* The nodal precursor acting via activin receptors induces mesoderm by maintaining a source of its convertases and BMP4. *Dev. Cell* **11**, 313–323 (2006).
7. ten Berge, D. *et al.* Wnt signaling mediates self-organization and axis formation in embryoid bodies. *Cell Stem Cell* **3**, 508–518 (2008).
8. Drukker, M. *et al.* Isolation of primitive endoderm, mesoderm, vascular endothelial and trophoblast progenitors from human pluripotent stem cells. *Nat. Biotechnol.* **30**, 531–542 (2012).
9. Blauwkamp, T.A., Nigam, S., Ardehali, R., Weissman, I.L. & Nusse, R. Endogenous Wnt signalling in human embryonic stem cells generates an equilibrium of distinct lineage-specified progenitors. *Nat. Commun.* **3**, 1070 (2012).
10. Peerani, R. *et al.* Niche-mediated control of human embryonic stem cell self-renewal and differentiation. *EMBO J.* **26**, 4744–4755 (2007).
11. Bauwens, C.L. *et al.* Control of human embryonic stem cell colony and aggregate size heterogeneity influences differentiation trajectories. *Stem Cells* **26**, 2300–2310 (2008).
12. Sakai, Y., Yoshiura, Y. & Nakazawa, K. Embryoid body culture of mouse embryonic stem cells using microwell and micropatterned chips. *J. Biosci. Bioeng.* **111**, 85–91 (2011).
13. James, D., Levine, A.J., Besser, D. & Hemmati-Brivanlou, A. TGFβ/activin/nodal signaling is necessary for the maintenance of pluripotency in human embryonic stem cells. *Development* **132**, 1273–1282 (2005).
14. Xu, R.-H. *et al.* NANOG is a direct target of TGFβ/activin-mediated SMAD signaling in human ESCs. *Cell Stem Cell* **3**, 196–206 (2008).
15. Sato, N., Meijer, L., Skaltsounis, L., Greengard, P. & Brivanlou, A.H. Maintenance of pluripotency in human and mouse embryonic stem cells through activation of Wnt signaling by a pharmacological GSK-3-specific inhibitor. *Nat. Med.* **10**, 55–63 (2004).
16. Yu, P., Pan, G., Yu, J. & Thomson, J.A. FGF2 sustains NANOG and switches the outcome of BMP4-induced human embryonic stem cell differentiation. *Cell Stem Cell* **8**, 326–334 (2011).
17. Amita, M. *et al.* Complete and unidirectional conversion of human embryonic stem cells to trophoblast by BMP4. *Proc. Natl. Acad. Sci. USA* **110**, E1212–E1221 (2013).
18. Sudheer, S., Bhushan, R., Fauler, B., Lehrach, H. & Adjaye, J. FGF inhibition directs BMP4-mediated differentiation of human embryonic stem cells to syncytiotrophoblast. *Stem Cells Dev.* **21**, 2987–3000 (2012).
19. Li, Y. *et al.* BMP4-directed trophoblast differentiation of human embryonic stem cells is mediated through a ΔNp63$^+$ cytotrophoblast stem cell state. *Development* **140**, 3965–3976 (2013).
20. Bernardo, A.S. *et al.* BRACHYURY and CDX2 mediate BMP-induced differentiation of human and mouse pluripotent stem cells into embryonic and extraembryonic lineages. *Cell Stem Cell* **9**, 144–155 (2011).

21. Loh, K.M. & Lim, B. A precarious balance: pluripotency factors as lineage specifiers. *Cell Stem Cell* **8**, 363–369 (2011).
22. Thomson, M. *et al.* Pluripotency factors in embryonic stem cells regulate differentiation into germ layers. *Cell* **145**, 875–889 (2011).
23. Teo, A.K.K. *et al.* Pluripotency factors regulate definitive endoderm specification through eomesodermin. *Genes Dev.* **25**, 238–250 (2011).
24. Wang, Z., Oron, E., Nelson, B., Razis, S. & Ivanova, N. Distinct lineage specification roles for NANOG, OCT4, and SOX2 in human embryonic stem cells. *Cell Stem Cell* **10**, 440–454 (2012).
25. Li, L. *et al.* Location of transient ectodermal progenitor potential in mouse development. *Development* **140**, 4533–4543 (2013).
26. Chawengsaksophak, K., de Graaff, W., Rossant, J., Deschamps, J. & Beck, F. Cdx2 is essential for axial elongation in mouse development. *Proc. Natl. Acad. Sci. USA* **101**, 7641–7645 (2004).
27. Williams, M., Burdsal, C., Periasamy, A., Lewandoski, M. & Sutherland, A. Mouse primitive streak forms *in situ* by initiation of epithelial to mesenchymal transition without migration of a cell population. *Dev. Dyn.* **241**, 270–283 (2012).
28. Ng, V.Y., Ang, S.N., Chan, J.X. & Choo, A.B.H. Characterization of epithelial cell adhesion molecule as a surface marker on undifferentiated human embryonic stem cells. *Stem Cells* **28**, 29–35 (2010).
29. Inman, G.J. *et al.* SB-431542 is a potent and specific inhibitor of transforming growth factor-β superfamily type I activin receptor-like kinase (ALK) receptors ALK4, ALK5, and ALK7. *Mol. Pharmacol.* **62**, 65–74 (2002).
30. Bachiller, D. *et al.* The organizer factors Chordin and Noggin are required for mouse forebrain development. *Nature* **403**, 658–661 (2000).
31. Perea-Gomez, A. *et al.* Nodal antagonists in the anterior visceral endoderm prevent the formation of multiple primitive streaks. *Dev. Cell* **3**, 745–756 (2002).
32. Behringer, R.R., Wakamiya, M., Tsang, T.E. & Tam, P.P. A flattened mouse embryo: leveling the playing field. *Genesis* **28**, 23–30 (2000).
33. Tam, P.P.L. & Gad, J.M. in *Gastrulation: From Cells to Embryo* (ed. Stern, C.D.) Ch. 16 (CSHL Press, 2004).
34. Hwang, Y.-S. *et al.* Microwell-mediated control of embryoid body size regulates embryonic stem cell fate via differential expression of WNT5a and WNT11. *Proc. Natl. Acad. Sci. USA* **106**, 16978–16983 (2009).
35. Moledina, F. *et al.* Predictive microfluidic control of regulatory ligand trajectories in individual pluripotent cells. *Proc. Natl. Acad. Sci. USA* **109**, 3264–3269 (2012).
36. Eiraku, M. *et al.* Self-organizing optic-cup morphogenesis in three-dimensional culture. *Nature* **472**, 51–56 (2011).
37. Lancaster, M.A. *et al.* Cerebral organoids model human brain development and microcephaly. *Nature* **501**, 373–379 (2013).
38. Sato, T. *et al.* Single Lgr5 stem cells build crypt-villus structures *in vitro* without a mesenchymal niche. *Nature* **459**, 262–265 (2009).
39. Sato, T. & Clevers, H. Growing self-organizing mini-guts from a single intestinal stem cell: mechanism and applications. *Science* **340**, 1190–1194 (2013).
40. Spence, J.R. *et al.* Directed differentiation of human pluripotent stem cells into intestinal tissue *in vitro*. *Nature* **470**, 105–109 (2011).

ONLINE METHODS

Cell culture. All experiments detailed in the main text were performed with the RUES2 hESC line derived in our laboratory and described previously. The patterning experiment in **Figure 2** was also performed with the RUES1 and H1 cell lines (**Supplementary Fig. 9**). For routine culture for maintenance, all hESC lines were grown in HUESM medium that was conditioned by mouse embryonic fibroblasts (MEF-CM) and supplemented with 20 ng/ml bFGF. Cells were tested for mycoplasma before beginning experiments and then again at 2-month intervals. Cells were grown on tissue culture dishes coated with Matrigel (BD Biosciences, 1:40 dilution). Dishes were coated in Matrigel overnight at 4 °C and then incubated at 37 °C for 1 h immediately before the cells were seeded on the surface.

For micropatterned cell culture, micropatterned glass coverslips (CYTOO) were first coated with 50 μg/ml poly(D-lysine) in H_2O (PDL; Millipore) for 2 h. The PDL was then removed by serial dilutions without allowing the coverslip to dry (dilution 1:4 in H_2O, six times), before two complete washes were performed with H_2O. Coverslips were then incubated with Matrigel (1:100 dilution in DMEM-F12) overnight at 4 °C. Before cell seeding, the Matrigel was removed with serial dilutions in ice-cold PBS (dilution 1:4, six times) before two complete washes in ice-cold PBS. Cells already resuspended in growth medium were seeded onto the coverslips immediately following the removal of the PBS. We found it was important to take care to keep the coverslips at 4 °C at all times when in Matrigel solution and to ensure that the coverslips were not allowed to dry at any time after the application of the Matrigel. Both polymerization and drying of the Matrigel led to inconsistent cell adhesion with cells more likely to detach from the surface during the experiment.

Cell seeding onto micropatterned coverslips was performed as follows. Cells growing in MEF-CM and FGF were pretreated with the Rock-inhibitor Y27632 (Rock-I; 10 μM) for 1 h, washed once with PBS, and dissociated with trypsin. Cells were centrifuged, 5×10^5 cells were resuspended in 2.5 ml of growth medium containing Rock-I, and the entire solution was placed over the coverslip in a 35-mm tissue culture dish. After 2 h, the medium was replaced with MEF-CM without Rock-I, and cells were incubated overnight.

We also tested the effects of using the chemically defined mTeSR1 culture medium rather than MEF-CM and obtained similar patterns upon treatment with BMP4 to those presented here (**Supplementary Fig. 9**). However, we found that MEF-CM better promoted adhesion to the micropatterned surface, and it was therefore used in all subsequent experiments. Finally, we tested the effects of growing cells on recombinant Laminin-521 (Biolamina) rather than Matrigel, and again obtained similar patterns (**Supplementary Fig. 9**). Laminin-521 coating of coverslips was performed as follows. Coverslips were coated with 5 μg/ml of Laminin-521 diluted in PBS with calcium and magnesium for 2 h at 37 °C. Laminin was then removed with six serial dilutions in warm PBS (dilution 1:4) before two complete washes in PBS. Cells were then seeded as described above for the PDL-Matrigel–coated coverslips.

siRNA experiments. Cells were passaged as single cells in Rock-I into 35-mm dishes at a density of 200,000 cells per dish. The next day, cells were transfected with siRNA (Ambion Silencer Select) using RNAiMax (Invitrogen). The final concentration of siRNA was 20 nM, and 2.5 μl of RNAiMax were used for each dish. The following day, cells were seeded onto micropatterned coverslips and differentiation experiments were performed as described above.

PDMS microwells. Molds to create PDMS wells of controlled diameter and depth were designed using a 3D CAD software (Autodesk Inventor) and then 3D printed (3D Systems ProJet 3510 HD Plus printer). The smallest wells that this technique allowed us to make reliably were 250 μm in diameter and 250 μm in depth. We found that boiling the 3D-printed parts in water containing 1% Triton X-100 for 4 h was necessary to allow the PDMS to cure on the 3D-printed parts. Molds were filled with PDMS (10:1 base:reticulant) and degassed under vacuum. In order to create opened wells, the mold was placed between two glass slides on which pressure was applied, typically with a large paper clip. After PDMS curing at 80 °C for several hours, the PDMS wells were unmolded and boiled in distilled water to ensure sterility and that all PDMS was cured. PDMS wells were then washed with ethanol and dried in a cell culture cabinet to keep them sterile.

Wells were then stuck on the dry cell culture substrate (either glass coverslips, regular tissue culture dish, or optically clear plastic dishes (Ibidi)). The wells were then coated with cell adhesion–promoting proteins in either a one-step protocol (Laminin-521) or a two-step protocol (PDL followed by Matrigel). To remove bubbles trapped in wells, we centrifuged the PDMS wells filled with the coating solution (630*g*, 2 min). After the necessary incubation time, the coating solution was aspirated and cells were seeded.

Immunofluorescence. Coverslips were rinsed once with PBS, fixed with 4% paraformaldehyde, rinsed twice with PBS, and then blocked and permeabilized with 3% donkey serum and 0.1% Triton X-100 in PBS for 30 min. When performing immunofluorescence for pSmad1, we pretreated cells with 1% SDS in PBS for 30 min at 37 °C before blocking. Coverslips were incubated with primary antibodies overnight at 4 °C (for primary antibodies and dilutions, see **Supplementary Table 1**), washed three times in PBS for 30 min each wash, incubated with secondary antibodies (Alexa 488, Alexa 555 or Alex 647 conjugated (Molecular Probes); dilution 1:500) and DAPI nuclear counterstain for 30 min, and then washed twice with PBS. Coverslips were mounted on slides using Fluoromount-G mounting medium (Southern Biotech).

Imaging. All wide-field images were acquired on an Olympus IX71 inverted microscope with a 20×, 0.75–numerical aperture (NA) lens. We used tiled image acquisition to acquire images of the entire coverslip (approximately 2,500 stage positions per coverslip) in four channels corresponding to DAPI and Alexa 488, Alexa 555 and Alexa 647–conjugated antibodies. All confocal images were acquired on a Leica SP8 inverted confocal microscope with a 40×, 1.1-NA water-immersion objective. 3D visualization and rendering was performed using Imaris software.

Image analysis. All image analysis was performed using custom software written in Matlab. Because we imaged the entire coverslip, we used the fact that we also imaging the regions without cells to create background and normalization images as follows.

We first took the pixel-by-pixel minimum and average across all images: $m = \min_j(I_j)$; $a = \text{mean}_j(I_j)$ where I_j represents the jth image. We then used m as a background image and defined a normalization image according to $n = (a - m)/\max(a - m)$, where the max is across all pixels in the image. The mean and normalization images were then smoothed with a Gaussian filter several times the size of a cell diameter, and each image was corrected according to $I_j \rightarrow (I_j - m)./n$ where the "./" represents pixelwise division. In general, subtracting m removes the (typically spatially homogeneous) camera noise, and dividing by n corrects for any inhomogeneities in the image due to the illumination or other factors.

After each image was corrected in this way, we identified and quantified the cells in each image using an algorithm that we described previously[41] (see "Marker quantification" below). Because larger colonies span multiple images, we preformed image alignment and used the resulting overlap between images to put the coordinates of each cell in "coverslip coordinates," resulting in a list of the position of every cell on the coverslip. We then separated these cells into colonies by computing the alphavol of the points using the Matlab function "alphavol" (http://www.mathworks.com/matlabcentral/fileexchange/28851-alpha-shapes) with a radius (r_v) of 100 pixels. The alphavol is similar in concept to a convex hull except that it will form separate boundaries for sets A and B if all points in set A are greater than r_v away from all points in set B. Having identified colonies, we classified them on the basis of their radius. For quantification of immunofluorescence, either we normalized the intensity to the DAPI intensity in the same cell or, for proteins that translocate to the nucleus upon activation, we normalized the nuclear intensity to the cytoplasmic intensity in the same cell. Both of these normalizations serve to remove imaging artifacts.

Marker quantification. Individual cells were identified in images and quantified for markers as described previously[41]. All marker intensities were normalized to the DAPI intensity in the same cell with the exception of SMAD2, where we normalized the nuclear SMAD2 intensity to the cytoplasmic intensity in the same cell. We have found this nuclear-to-cytoplasmic ratio to be a sensitive metric for signaling activity[41]. Radial averages were performed over all colonies on the micropatterned coverslip ($n = 25$ for 1,000-μm colonies, $n = 144$ for 500-μm colonies and $n = 576$ for 250-μm colonies), and the error bars given shown are s.d. between colonies. Each marker quantification was performed in at least two different independent experiments. For 500-μm and 1,000-μm colonies, we manually excluded those colonies in which cell seeding was uneven (for example, large empty areas within the micropatterned patch).

41. Warmflash, A. *et al.* Dynamics of TGF-β signaling reveal adaptive and pulsatile behaviors reflected in the nuclear localization of transcription factor SMAD4. *Proc. Natl. Acad. Sci. USA* **109**, E1947–E1956 (2012).

doi:10.1038/nmeth.3016